Chemical Engineering Journal 426 (2021) 131909

Contents lists available at ScienceDirect

Chemical Engineering Journal

journal homepage: www.elsevier.com/locate/cej

Role of the organic loading rate and the electrodes' potential control strategy on the performance of a micro pilot tubular microbial electrolysis cell for biogas upgrading

Lorenzo Cristiani *, Marco Zeppilli, Marianna Villano, Mauro Majone

Department of Chemistry University of Rome Sapienza, Piazzale Aldo Moro 5, 00185 Rome, Italy

ARTICLE INFO

Keywords:
Biogas Upgrading
Microbial electrolysis cell
Bioelectromethanogenesis
Reaction overpotentials

ABSTRACT

An innovative biogas upgrading process consists in the utilization of a microbial electrolysis cell (MEC) in which a biocathode performs the bioelectromethanogenesis reaction reducing the CO_2 into CH_4 while an additional CO_2 removal mechanism consists in the CO_2 sorption as HCO_3^-, due to alkalinity generation in the catholyte. Here, a two chamber 12-liter tubular MEC has been developed to upgrade biogas by using bioelectrochemical organic matter oxidation at the anode to partially sustain the energy demand of the process. In the tubular MEC, the electroactive microorganisms' selection was obtained by polarizing the anode chamber at + 0.2 V vs. SHE (Standard Hydrogen Electrode). Under this condition, three values of the applied organic loading rate (OLR) have been investigated. Once the best OLR was selected at 2.55 gCOD/Ld, the potentiostatic control of the tubular MEC was switched from the anode to the cathode. As reported in a previous experiment, the potentiostatic control shift resulted in a sharp decrease of the process' energy consumption thanks to minimization of the anodic overpotential. Moreover, three different runs were conducted with the cathodic potential controlled at −1.3 V; −1.8 V; −2.3 V vs. SHE to investigate the performances of the CO_2 abatement. The lowest energy consumption for CO_2 removal was obtained during the −1.3 V vs SHE condition with a consumption of 0.5 kWh/Nm^3 of removed CO_2. Those results indicate that the potentiostatic control switch from the anode to the cathode permits to minimize the energy consumption of a micro pilot MEC having a tubular configuration.

1. Introduction

The growing energetic demand needs to be answered with renewable resources due to the unsustainability of the traditional fuels' production. The European Union decided to stake on many technologies to produce renewable energy [1]. The anaerobic digestion (AD) is one of the most consolidated technologies to reuse organic wastes [2]. The main product of AD is the biogas; a gas mixture mainly composed by carbon dioxide and methane [3]. To obtain biomethane, with a high percentage of methane (>95%), it is necessary a purification step to remove the impurities such as NH_3, H_2S, as well as an upgrade step to remove the CO_2 [4 5]. Biogas is already a large industry that continues to grow. The present upgrading technologies, that is first-generation upgrading, are implemented at a commercial level. The increasing market share indicates that the industry is open for new technologies [6]. Furthermore, the use of upgraded biogas in transport applications has increased as result of the new opportunities for the use of biogas and benefited from various support schemes and programs. Technological improvements in biogas upgrading technologies to biomethane could lead to lower energy intensity and improved cost performance that could make biomethane cost competitive with fossil fuel use in transport [7]. A way to enhance the percentage of methane is to catalytically reduce CO_2 into CH_4, however, the high operational costs and the cost of the catalyst force to resort to other strategies like pressure swing adsorption, membrane separation, cryogenic separation and biological methane enrichment [4]. The microorganisms catalyse the CO_2 reduction exploiting the reducing power of hydrogen, though, its costs and its source force to look for an alternative strategy [8]. An innovative strategy for biogas upgrading consists in the utilization of a microbial electrolysis cell (MEC) in which the reduction of carbon dioxide to methane is performed by a biocathode. MEC is a type of bioelectrochemical systems (BES), which exploit the extracellular electron transfer mechanism used by the electroactive microorganisms to employ the electrode as electron acceptor or donor [9]. If the biofilm adherent at the solid electrode uses

* Corresponding author.
E-mail address: lorenzo.cristiani@uniroma1.it (L. Cristiani).

https://doi.org/10.1016/j.cej.2021.131909
Received 5 May 2021; Received in revised form 16 July 2021; Accepted 15 August 2021
Available online 21 August 2021
1385-8947/© 2021 The Author(s). Published by Elsevier B.V. This is an open access article under the CC BY license (http://creativecommons.org/licenses/by/4.0/).

the electrode as electron donor, this system can be named biocathode, on the contrary the system composed by a biofilm which uses the solid electrode in absence of oxygen as final electrode acceptor can be named bioanode [10]. Biocathodes can be utilized for many applications, including environmental bioremediation [11 12] and chemical synthesis [13]. The importance of the biocathode in this kind of processes is confirmed by the amount of studies present in the literature focused on the materials[14 15 16], on the potentials [17], on size [18], on the conditions [19] and on the microorganisms [20 21] which are responsible of the processes. The bioelectromethanogenesis could be obtained using an electrode acting as a donor of electrons for the reduction of CO_2 into CH_4 [22]; this reduction could be performed through two different metabolic pathways: hydrogen mediated, were the hydrogen is produced and used by hydrogenotrophic methanogens to reduce CO_2 into CH_4 [23], or directly by an electron uptake mediated by particular membrane proteins and/or conductive pili [24]. To reduce CO_2 to CH_4 or other reduced products an external potential must be applicated to obtain the needed reducing power. Several studies were made to couple a bioanodic oxidation reaction to the cathodic reducing reaction to lower the energetic consumption needed to apply the electric potential. Moreover, a second but more significant CO_2 removal mechanism, further than its reduction, was studied inside a MEC's cathodic chamber, which exploits the alkalinity generation due to the bioelectromethanogenesis. The alkalinity inside the cathodic chamber is generated by the usage of protons, for either hydrogen or methane generation, and the transport of ionic species through the membrane different from the protons or the hydroxyls, [25] i.e., the alkalinity generation permits the removal of 9 mol of CO_2 for each mole of CH_4 produced by the biocathode. Furthermore, many studies suggested to use a BES to upgrade a biogas outcoming from an anaerobic digestor exploiting its double mechanism to remove CO_2 from a gaseous mixture [26]. Here, a 12L micropilot tubular MEC has been assembled to be integrated with an anaerobic digestion process in which biogas upgrading is performed inside the cathodic chamber along with the COD oxidation inside the anodic chamber. In a previous study [27], the operation of the tubular MEC was tested by either applying a fixed potential difference between the anode and the cathode or by controlling the anode potential at a fixed value of + 0.2 V vs. SHE (Standard Hydrogen Electrode), with the latter condition resulting in a better performance in terms of both andic COD removal and cathodic CO_2 abatement. Considering these results, in this study, the operation of the tubular MEC with the anode controlled at + 0.2 vs SHE has been explored at three different organic loading rates, by changing the concentration of the feeding solution made of a synthetic mixture of organic acids with a composition simulating the one of a typical digestate. Whereupon, following a previous experiment performed in a bench scale filter press MEC [28], the polarization was switched from controlling the anodic potential to controlling the cathodic potential, in order to promote the minimization of the anodic overpotentials and consequently an important decrease of the energy consumption of the process. Overall, the effect of three cathodic potential values were investigated to verify the possibility to enhance the performance of the overall process. Afterwards, a deep characterization of the tubular MEC potential loss as well as a detailed analysis of the COD and CO_2 removal including the energetic demand for each applied operating condition have been performed. Also, the specific energetic consumption for COD and CO_2 removal were compared with the benchmark technologies' consumption, i.e., activated sludge for COD removal and water scrubbing for biogas upgrading.

2. Material and methods

2.1. Tubular pilot-scale MEC set up

The tubular pilot scale MEC consisted in a plexiglass cylindric reactor of 12 L, the inner anodic (3.14L) chamber was separated from the cathodic chamber (8.86L) by an anion exchange membrane (AEM, FAD FUMASEP, FumatechGmbH). Both anodic and cathodic chambers were filled with graphite granules presenting a bed porosity of 0.57; the anodic chamber was equipped with a sampling-glass chamber for the liquid sample collection while the cathodic chamber, was equipped with a sampling-glass chamber for the liquid and the gas sample collection. A schematic representation of the tubular MEC used in this study is reported in Fig. 1. In principle, the developed pilot scale MEC can be easily combined with an anaerobic digestion process (consisting of either one or two stages) to upgrade the biogas while using the digestate as a source of electrons [12]. The inner anodic chamber was inoculated using 1 L of activated sludge (6.5 ± 0.1 gVSS/L) coming from a wastewater treatment plant, while the outer cathodic chamber was inoculated with 4 L of an anaerobic sludge (4.3 ± 0.1 gVSS/L) coming from a thermophilic anaerobic digester. Using a peristaltic pump, the anode was fed in continuous-flow mode at an average flow rate of 6.9 ± 0.1 L/d, the result is a hydraulic retention time (HRT) of 11 h. The mineral medium (MM) was composed of: NH_4Cl (0.125 g/L), $MgCl_2{\cdot}6H_2O$ (0.1 g/L), K_2HPO_4 (4 g/L), $CaCl_2{\cdot}2H_2O$ (0.05 g/L), 10 mL/L of a metal solution, and 1 mL/L of a vitamin solution. Volatile fatty acids (VFAs) were added to the feeding solution to simulate the COD fraction of a fermented wastewater. Three values of the applied organic loading rate (OLR) were explored by changing the VFA concentration in the feeding solution. During the run at an OLR of 2.55 gCOD/Ld, the VFA concentration was (g/L): acetate (0.47), propionate (0.165) and butyrate (0.138). Successively, for the 3.82 gCOD/Ld and the 5.11 gCOD/Ld runs, the VFA concentrations were enhanced by the 50% and by the 100%, respectively. The cathodic chamber was continuously fed with a gaseous mixture composed of CO_2 at 30% (v/v) and N_2 at 70% to simulate the CO_2 content of a typical biogas. The gaseous phases were sampled by a 11 mL glass vial sealed with butyl rubber caps while a digital barometer was used to determine the operating pressures of the gaseous samples. The catholyte was continuously recirculated inside the cathodic chamber using a peristaltic pump. The water electroosmotic diffusion through the AEM lowered the liquid level inside the cathodic chamber, forcing a daily refill with MM. The reactor operated at controlled laboratory temperature of 25 °C. The tubular MEC was operated by a three electrodes configuration through an Ag/AgCl reference electrode (+0.2 V vs. SHE) and an AMEL model 549 potentiostat. During the anodic potentiostatic operation the anode was used as working electrode while during the cathodic potentiostatic control, the cathode acted as working electrode, both anode and cathode chamber were equipped with an Ag/AgCl reference electrode which was used to measure the counter electrode potential, i.e., the cathode potential during the anodic potentiostatic control while the anode potential during the cathodic potentiostatic control. Two digital multimeters (Aim-TTI 1604) were connected to measure the flowing current and the potential difference between the two electrodes.

2.2. Analytical procedures

The chemical oxygen demand (COD) was calculated multiplying the theoretical conversion factor (1.067 $mgCOD/mg_{acetate}$; 1.51 $mgCOD/mg_{propionate}$; 1.82 $mgCOD/mg_{butyrate}$) by the VFAs concentration measured with a gas-chromatograph (DaniMaster, stainless-steel column packed with molecular sieve; He as carrier gas 18 mL/min; oven temperature 175 °C; flame ionization detector (FID) temperature 200 °C). The methane content of the gas phase has been analysed, sampling 50 μL of the headspace of the compartments by a gas-tight Hamilton syringe and injecting it into a Varian (Lake Forest, CA, USA) 3400 gas-chromatograph (GC; 2 m × 2 mm glass column packed with 60/80 mesh Carbopack B/1% SP-1000; He carrier gas at 18 mL/min; oven temperature at 50 °C; FID temperature 200 °C); on the other hand, the CO_2 and H_2 determination has been performed by injecting 50 μL of gaseous sample into a DaniMAster gaschromatograph (stainless-steel column packed with molecular sieve; He as carrier gas 18 mL/min; oven

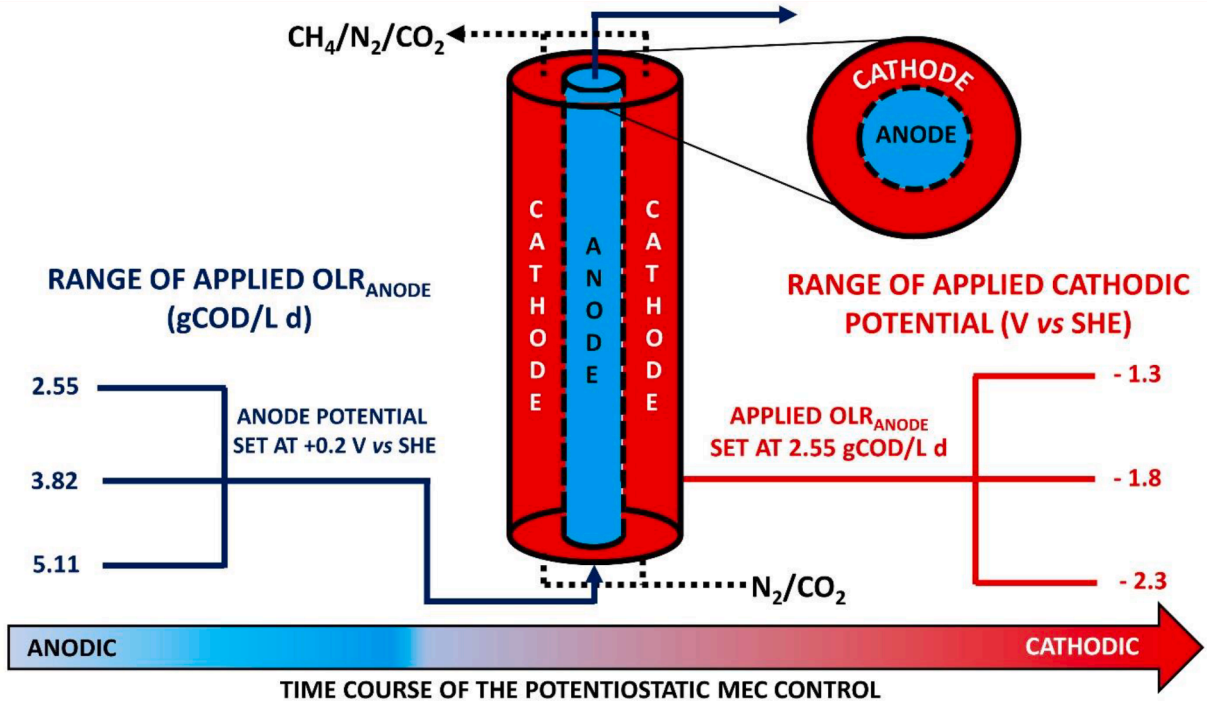

Fig. 1. Schematic representation of the studied MEC.

temperature 70 °C; thermal-conductivity detector (TCD) temperature 150 °C). The inorganic carbon was measured by TOC (Total Organic Carbon Analyzer)-V CSN (Shimadzu) on filtered samples (0.2 μm). The concentration of volatile suspended solids (VSS) was measured using GF/C filter (47 mm diameter, 1 μm porosity) following the APHA-AWWA-WPCF (1992) procedure.

2.3. Theoretical computations

The removed COD is calculated by multiplying the flow rate by the difference between the concentration inside the feeding solution and the outcoming solution, as reported by the eq. (1).

$$COD_{removed} = F^{*}(COD_{in} - COD_{out}) \quad (1)$$

in which COD_{in} (mg/L) and COD_{out} (mg/L) represent respectively the anodic influent and effluent COD while F(L/d) is the influent and effluent flow rate in the anodic chamber (L/d). The efficiency for COD removal was calculated with the equation (2).

$$COD_{removalefficiency} = \frac{(COD_{in} - COD_{out})}{COD_{in}} \quad (2)$$

The COD converted into electric current was expressed as electrons' equivalents, considering the water oxidation reaction (equation (3).)

$$2H_2O \rightarrow O_2 + 4e^- + 4H^+ \quad (3)$$

The meq_{COD} was calculated by using a theoretical conversion factor of 4 meq/32 mgO_2.

The Coulombic Efficiency (CE%) represents the amount of COD converted into current by its oxidation; it was evaluated as the ratio between the registered electric current and the theoretical electric current producible with the measured COD removal.

$$CE = \frac{meq_i}{meq_{COD}} \quad (4)$$

The cumulative electric charge (meqi) was calculated by integrating the current (A) over time and dividing it by the Faraday's constant (F = 96485C/eq).

The methane production rate $rCH_{4(mmol)}$ (mmol/d) was also expressed in terms of equivalents $rCH_{4(eq)}$ (meq/d), considering the theoretical conversion factor of 8 meq/$mmol_{CH4}$, which was computed following the semi-reaction (5).

$$CO_2 + 8e^- + 8H^+ \rightarrow CH_4 + 2H_2O \quad (5)$$

$$rCH_{4(mmol)}{}^{*}8 = rCH_{4(meq)} \quad (6)$$

The Cathode Capture Efficiency (CCE, %) is the fraction of the flowing electric current diverted into a reduced product (methane, acetic acid) inside the cathodic chamber. It was calculated by the ratio between the cumulative equivalents of produced methane (meq_{CH4}) in a fraction of time and the cumulative electric charge flowed in the MEC during the same fraction of time:

$$CCE = \frac{meq_{CH4}}{meq_i} \quad (7)$$

The energy efficiency (ηE) was calculated considering the energy theoretically recoverable from the combustion of the produced methane (W_{CH4}) and the energetic consumption of the system (W_{in}):

$$\eta E = \frac{W_{CH4}}{W_{in}} = \frac{r_{CH4(mmol)} \times \Delta G_{CH4}}{\Delta V \times i} \quad (8)$$

where ΔGCH_4 (-817.97 KJ/mol) and $rCH_{4(mmol)}$ (mmol/d) represent the molar Gibbs free energy for methane combustion and the methane production rate, respectively; ΔV is the difference of potential established between the counter and the working electrodes (i.e., cell voltage), and i represents the average current flowing in the reactor expressed as Coulombs and calculated by integrating the flowing electric current over time.

To calculate the energetic consumption of the main process, the ΔCO_2 was transformed from mmol/d into Nm^3 following this equation.

$$\Delta CO_{2\left(\frac{Nm3}{d}\right)} = \frac{\Delta CO_{2}\left(\frac{mmol}{d}\right)}{1000} * \frac{24,4\left(\frac{NL}{mol}\right)}{1000}$$

where ΔCO_2 is the daily removal of CO_2 (Nm^3/d or mmol/d), 24,4 are

the number of litre that a mole occupies in normal conditions (20 °C/293,15 K and 1 atm/101,325 kPa, normal temperature and pressure)

The energetic consumptions were determined as follows.

$$\frac{kWh}{kgCOD_{removed}} = \frac{\Delta V*i*24(h/d)}{COD_{removed(kg/d)}}$$

$$\frac{kWh}{\Delta CO_{2(Nm3/d)}} = \frac{\Delta V*i*24(h/d)}{\Delta CO_{2(Nm3/d)}}$$

where ΔCO_2 is the daily removal of CO_2 (Nm^3/d), ΔV is the potential difference measured between anode and cathode (V), i is the electric current registered (A).

2.4. Potential loss characterization and overpotentials determination

Table 1. summarizes the parameters involved in overpotential estimation, moreover, Table 2. reports the different equilibrium semi-reactions utilized for the evaluation of the overpotentials of the anodic and cathodic reactions.

2.5. Inorganic carbon mass balance

The daily removal of CO_2 (ΔCO_2, mmol/d) inside the cathodic chamber has been evaluated by the equation (10).

$$\Delta CO_2 = Qcat_{in}*CO_{2in} - Qcat_{out}*CO_{2out} \quad (10)$$

in which Q_{cat}in (L/d) and Q_{cat}out (L/d) are the influent and effluent gas flow rates, respectively. Instead, CO_2in and CO_2out (mmol/L) represent the CO_2 concentrations in the feeding and effluent gaseous cathodic streams, respectively.

To make a balance it was considered that the inorganic carbon was present in many forms (i.e., CO_2 and HCO_3^- ion) inside the system, that the methane production and the CO_2 sorption (as HCO_3^- ion in the cathodic liquid phases) were the main cathodic CO_2 removal mechanisms. The HCO_3^- ion in the cathodic chamber is removed by the migration of HCO_3^- ion to the anodic chamber through the AEM membrane.

The equation (11) represents the IC mass balance for the system:

$$\Delta CO_2 = r_{CH4(mmol)} + HCO^-_{3transf} \quad (11)$$

The term $rCH_{4(mmol)}$ (mmol/d) represents the production rate of methane while $HCO_3^-{}_{trans}$ indicates the bicarbonate daily transferred from the anode to the cathode due to charge transport.

$rCH_{4(mmol)}$ was determined considering the measured concentration of CH_4 inside the gaseous outlet (mmol/L), the gaseous flow (L/d), the time passed between the measures and the total operational time.

$$r_{CH_4} = \frac{\sum_0^n([CH_4]_n*Qcat_{(out)n}*\Delta t_n)}{\Delta t_{tot}} \quad (12)$$

It is possible to calculate the IC recovery considering those two mechanisms as responsible of the IC removal.

$$ICrecovery\% = \frac{r_{CH4(mmol)} + HCO^-_{3transf}}{\Delta CO_2} x100 \quad (13)$$

The ionic transport contribution of the HCO_3^- to the electroneutrality maintenance, is calculated measuring the difference between the concentration of HCO_3^- inside the effluent and influent of the anodic chamber.

$$HCO^-_{3(transf)} = F*HCO^-_{3(out)} - HCO^-_{3(in)}) \quad (14)$$

afterward, is possible to convert the molar daily amount of HCO_3^- transferred in terms of current by

$$HCO^-_3(mA) = HCO^-_3(transf)*n*\frac{F}{86400} \quad (15)$$

where n is the charge of the bicarbonate ion (-1), F is the Faraday constant and 86400 represents the seconds in a day.

Table 1
Parameters involved in the overpotential estimation.

	Parameter Description	Parameter calculation
$E_{an(eq)}$	Equilibrium potential of the anode calculated according to table 2	
$E_{cath(eq)}$	Equilibrium potential of the cathode calculated according to table 2	
$E_{an(meas)}$	Measured potential vs reference electrode placed in the anode	
$E_{cath(meas)}$	Measured potential vs reference electrode placed in the cathode	
$\Delta V_{(meas)}$	Calculated potential difference according to the equation	$\Delta V_{(meas)} = E_{cath(meas)} - E_{an(meas)}$
$\Delta V_{(exp)}$	Measured potential difference between anode and cathode	$\Delta V_{(exp)} = \Delta V_{(meas)} + \sum \eta$
$\sum \eta$	Cell overpotential: represent the sum of the overpotentials due to	$\sum \eta = \Delta V_{(exp)} - \Delta V_{(meas)}$
η_{an}	Anodic overpotential	$\eta_{an} = E_{an(meas)} - E_{an(eq)}$
η_{cath}	Cathodic overpotential	$\eta_{cath} = E_{cath(meas)} - E_{cath(eq)}$

Table 2
Equilibrium reactions utilized for the overpotential estimation for anodic and cathodic reactions.

Semi-reaction	Nernst equation	E^0(V vs SHE)
$2HCO_3^- + 8e^- + 9H^+ \rightarrow CH_3COO^- + 2H_2O$	$E_{anCOD(eq)} = E^0 + \frac{RT}{8F}\ln\frac{[HCO_3^-]^2*[H^+]^9}{[CH_3COO^-]}$	+0.187
$O_2 + 4e^- + 4H^+ \rightarrow 2H_2O$	$E_{anO2(eq)} = E^0 + \frac{RT}{4F}\ln[pO_2]*[H^+]^4$	+1.23
$2H^+ + 2e^- \rightarrow H_2$	$E_{cath(eq)} = E^0 + \frac{RT}{2F}\ln\frac{[H^+]^2}{[pH_2]}$	0

3. Results and discussions

3.1. Potentiostatic control of the MEC anode: Effect of the organic loading rate

The MEC operation with the potentiostatic control of the anode was characterized by an initial start-up period, which consisted in both the anodic and cathodic liquid phases (containing the inocula and mineral medium) continuously recirculated. Moreover, after 3 days of operation the feeding solution made of VFA was supplied at the anolyte and refilled 15 days later. After the start-up period, which lasted 35 days, characterized by the potentiostatic control of the anode at + 0.2 V vs. SHE, the establishment of a stable electric current indicated the growth of an electroactive biofilm which was able to oxidize the organic matter using the anode as electron acceptor.

During the following period of the MEC operation with the anode potential controlled at + 0.2 V vs SHE, three operating conditions were explored whereby a different organic loading rate (OLR) was applied to the anode. During the three operating periods, the anodic chamber was continuously fed with the VFA synthetic mixture at an average flow rate of 6.8 ± 0.6 L/d, corresponding to a hydraulic retention time (HRT) of 0.46 days. During the first operating period, with an OLR of 2.55 gCOD/Ld, the average electric current resulted 241 ± 16 mA. Considering an average COD removal of 1.4 ± 0.1 gCOD/d the fraction of COD transformed into electric current, defined as coulombic efficiency (CE), resulted 121 ± 7%. This value is particularly high, probably due to the extra oxidation of the acetate produced inside the cathodic chamber which migrated through the anionic membrane. The production rate of

acetate decreased during the experimental period, but during the first 50 days of operation a high concentration of acetate was detected inside the cathodic chamber confirming the presence of acetogenic microorganisms inside the cathodic inoculum. The only product detected in the gaseous outlet was CH_4 with a production rate of 11 ± 1 mmol/d. The fraction of electric current stored into methane, named cathodic capture efficiency (CCE), resulted on average 41 ± 1% indicating a relative low efficiency of the cathode. This result is only referred to the production of methane and does not consider the acetate production. The acetate production rate is impossible to estimate due its migration and diffusion through the anion exchange membrane.

During the second experimental period, characterized by an OLR of 3.82 gCOD/Ld and the control of the anodic potential at + 0.2 V vs SHE, the electric current did not raise along with the COD removal resulting 240 ± 25 mA and 3.5 ± 0.1 gCOD/d, respectively. In the meantime, the methane production rate raised to 16 ± 1 mmol/d (Fig. S1) corresponding to a CCE of 59 ± 1%. As reported in Fig. 2. a) during the third operational period, the electric current raised to an average value of 312 ± 28 mA. Considering a COD removal on average of 2.2 ± 0.1 gCOD/d the CE resulted 103 ± 4%. The CH_4 production rate decreased to an average value of 9 ± 1 mmol/d (Table 3.).

In each explored condition, the difference of potential established between the MEC cathode and anode (ΔV) was periodically measured (Fig. 2A), in order to calculate the potential loss of the system. Notably, this difference was comparable when the OLR of 2.55 and 3.82 gCOD/Ld were applied to the anode (i.e., −2.29 and −2.35 V, respectively), and it significantly increased (up to −3.85 V) at the highest investigated OLR.

Table 3
Bioelectrochemical parameters for the anodic and cathodic reactions during the three OLR explored under the MEC anodic potentiostatic control.

Organic loading rate (gCOD/Ld)	2.55	3.82	5.11
Current (mA)	241 ± 16	240 ± 25	312 ± 28
COD removed (gCOD/d)	1.4 ± 0.1	3.5 ± 0.1	2.2 ± 0.1
COD removal efficiency (%)	41 ± 1	46 ± 1	19 ± 1
Coulombic Efficiency (CE, %)	121 ± 7	49 ± 5	103 ± 4
Methane production (mmol/d)	11 ± 1	16 ± 1	9 ± 1
Cathodic Capture Efficiency (CCE, %)	41 ± 1	59 ± 1	25 ± 1

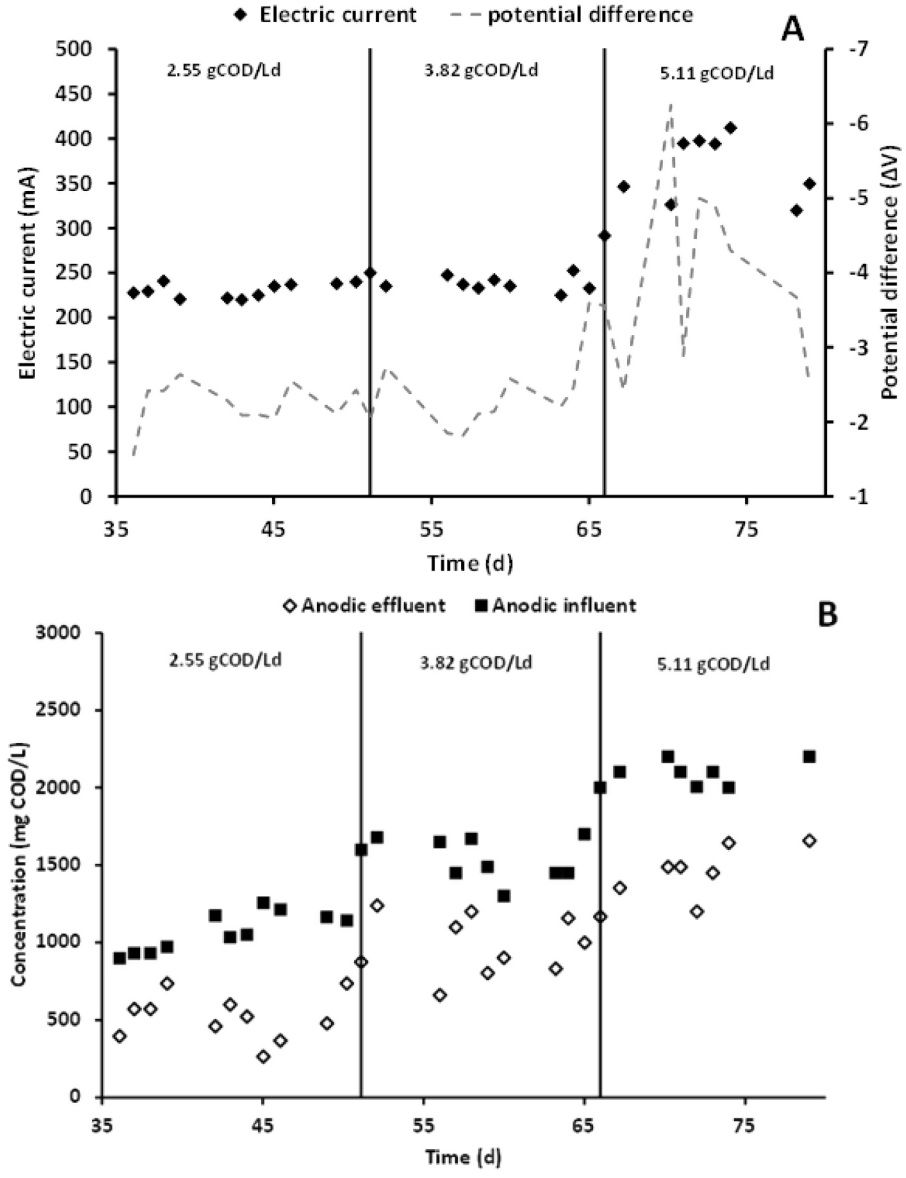

Fig. 2. MEC operation with the anode potential controlled at + 0.2 V (vs. SHE): a) Electric current and potential difference measured during the three operational periods, b) COD concentrations inside the anodic influent and effluent.

3.2. Potentiostatic control of the MEC cathode: Effect of the applied potential

After 95 days of the MEC operation, the potentiostatic control was switched from controlling the anodic potential at + 0.2 V vs SHE to controlling the cathodic potential and three values were tested. Initially, the cathode potential was set at −1.3 V vs SHE, a value selected considering the average value of the measured cathodic potential during the first two conditions performed by controlling the anode potential which resulted on average − 1.36 ± 0.23 V vs SHE. In correspondence to the switch of the potential control, the OLR applied to the MEC anode was decreased to 2.55 gCOD/Ld, due the better performance obtained with that specific OLR. During the − 1.3 V period the electric current resulted on average 91 ± 5 mA with a CE of 21 ± 1% due to a COD removal of 3.13 ± 0.03 gCOD/d (Figs. S2 and S3). About 118 ± 2% of the electric current was converted (i.e., CCE) into methane, giving a production rate of 12 ± 1 mmol/d. This considerably high value of the CCE can be explained by a non-electroactive production mechanism, probably an acetoclastic methanogenesis. A consequence of this mechanism is a non-electroactive COD removal and methane production as indicated by the low electric current generated in combination with a high COD removal and a high methane production. Those results were obtained also during the −1.8 V vs SHE period during which the cathodic potential was decreased by 0.5 V with the goal to increase the electric current flowing in the system. The COD removal resulted on average 5.2 ± 0.1 gCOD/d producing an electric current of 148 ± 5 mA and giving a CE of 20 ± 2%. As anticipated, under these conditions, the CCE resulted very high accounting for 191 ± 4% with a CH_4 production rate of 32 ± 2 mmol/d. During the first two cathodic potentiostatic conditions, as reported in Fig. 3, the average anodic potential resulted 0.49 and 0.48 V vs SHE, indicating the maintenance of the capacity of the bioanode to continue the oxidation of the COD by using the graphite as electron acceptor. Indeed, the detected potential resulted considerably lower than the potential necessary for water oxidation, which resulted 0.85 V vs SHE at the working anodic condition. Afterwards, the cathodic potential was further decreased by 0.5 V, resulting in a cathodic potential of −2.3 V vs SHE. Therefore, the electric current increased to 277 ± 8 mA, while the anodic COD removal decreased to 2.2 ± 1 gCOD/d giving an apparent CE of 88 ± 11%. As clearly showed in Fig. 3, by applying a potential of −2.3 V vs SHE, the anodic potential increased up to + 1.26 V vs SHE, indicating the establishment of the water oxidation reaction in the anodic chamber. The increase of the anodic potential was related to a kinetic limitation of the anodic reaction, i.e., being the anode the counter electrode chamber, the lack of electron production by the bioanode promoted the potential increase as reported in previous experiments [28]. However, being the water oxidation the electron-producing reaction, the CE of the anodic chamber was not considered. During this period, the methane production rate was 15 ± 1 mmol/d giving as a result a CCE of 48 ± 1% (Table 4.).

3.3. Characterization of the MEC potential loss

The shift of the potentiostatic control of the MEC from the anode to the cathode, as already described in the literature [28], promoted the shift of the electrochemical overpotential distribution between the two electrodes. Therefore, an analysis of the potentials was made to better understand and characterize the processes happening inside the MEC. This analysis is necessary to explain why the energetic consumptions are different. As reported in Table 5, the equilibrium potential of the cathodic reactions ($E_{cath(eq)}$) evaluated by the Nernst equation, remained −0.31 V vs SHE during all the conditions at different applied OLR with the anode potential controlled at + 0.2 V vs SHE, being stationary the concentration of all species involved in the cathodic reaction (i.e., pH and H_2 partial pressure). Differently, the anodic equilibrium potential resulted different between the anodic and cathodic potentiostatic conditions. Indeed, the average equilibrium potential during the three anodic conditions at different OLR reached the value of − 0.64 ± 0.03 V vs SHE (i.e., the acetate oxidation), while during the cathodic potentiostatic conditions, the equilibrium potential for the anodic reaction required a different evaluation influenced by the potential detected at

Table 4
Bioelectrochemical parameters for the anodic and cathodic reactions during the three explored conditions with the MEC cathodic potentiostatic control.

Cathodic potential (V vs SHE)	−1.3	−1.8	−2.3
Current (mA)	91 ± 5	148 ± 5	277 ± 8
COD removed (gCOD/d)	3.1 ± 0.1	5.2 ± 0.1	2.2 ± 0.1
Coulombic Efficiency (CE, %)	21 ± 1	20 ± 2	–
Methane production (mmol/d)	12 ± 1	32 ± 2	15 ± 1
Cathodic Capture Efficiency (CCE, %)	118 ± 2	191 ± 4	48 ± 1

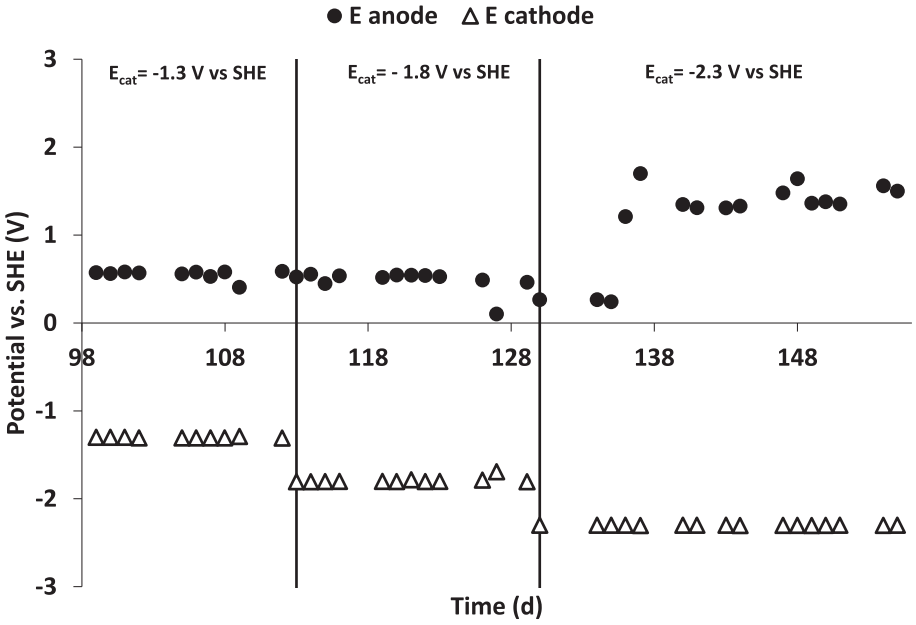

Fig. 3. Anodic and cathodic potential during the three operating periods of the MEC with the potentiostatic control of the cathode.

Table 5
Anodic and cathodic overpotential evaluation throughout all the operating periods explored of the MEC.

	Control of the anode potential			Control of the cathode potential		
	2.55 gCOD/Ld	3.82 gCOD/Ld	5.11 gCOD/Ld	−1.3 V vs SHE	−1.8 vs SHE	−2.3 vs SHE
$E_{an\ (meas)}$	0.22	0.22	0.23	0.49	0.48	1.26
$E_{cath\ (meas)}$	−1.30	−1.30	−2.49	−1.36	−1.79	−2.50
$E_{an\ (eq)}$	−0.66	−0.64	−0.63	0.06	0.05	0.75
$E_{cath\ (eq)}$	−0.31	−0.31	−0.31	−0.29	−0.30	−0.33
η_{an}	0.88	0.86	0.86	0.43	0.43	0.51
η_{cath}	−0.99	−1.00	−2.18	−1.08	−1.49	−2.17

the anodic chamber ($E_{an(meas)}$). During the first two cathodic potentiostatic conditions at − 1.3 and − 1.8 V vs SHE, the average anodic potential resulted + 0.49 ± 0.05 and + 0.48 ± 0.05 V vs SHE, respectively with an average increase of + 0.27 V with respect the anodic potentiostatic runs, in which the anodic chamber represented the working electrode which was controlled at + 0.2 V vs SHE. Being the potential of the anode not sufficient for the water oxidation reaction, as reported in the literature, the average potential between the acetate and water oxidation was used to determine the equilibrium potential of the reaction [29]. An average anodic equilibrium potential ($E_{an(eq)}$) of − 0.03 and − 0.02 V vs SHE was then adopted for the first two cathodic potentiostatic conditions, while during the last cathodic potentiostatic condition at − 2.3 V vs SHE, in which the anode potential reached + 1.26 V vs SHE, the ($E_{an(eq)}$) reached + 0.75 V vs SHE considering the water oxidation reaction (E^0 =+1.23 V vs SHE). According to previous literature works, the anodic and cathodic overpotentials were evaluated by the difference between the measured potential and the equilibrium potential. As reported in Table 5, during the three anodic potentiostatic conditions, the anodic overpotentials resulted similar, this evidence was directly correlated to the fact that the potentiostatic technique can be described as an "overpotential controlled technique". On the contrary, the shift of potentiostatic control from the anode to the cathode fixed the overpotential for the cathodic reaction, allowing the anodic potential to minimize spontaneously its overpotential according to its counter-electrode function. Indeed, the anodic overpotentials decreased from 0.86 V of the anodic potentiostatic condition to 0.43 and 0.51 V of the cathodic potentiostatic conditions. Differently, the cathodic overpotentials resulted almost constant under anodic and cathodic potentiostatic control, this effect can be explained by the fact that the potentiostatic cathodic condition was set based on the overpotential observed during the anodic potentiostatic control of the process in which the cathode acted as counter electrode and its overpotential was the minimum necessary for the anodic reaction sustainment.

The anodic and cathodic overpotentials description clearly showed that the evolution of the anodic reaction which maintained the ability to convert the COD into current, was addressed to the overpotential minimization. Moreover, as reported in Table 6 the cell overpotential (Ση), which represents the difference between the experimental cell voltage and the cell voltage evaluated by the measured anodic and cathodic potential, followed the anodic overpotential behaviour. Cell overpotentials are related to the resistance of the electrolyte and depends on the ions' concentration (i.e., conductivity) and mobility as well as on the presence of an ion exchange membrane to separate the two MEC compartments. Indeed, while during the anodic potentiostatic condition the overpotentials increased accordingly to the current, during the first two cathodic potentiostatic conditions (i.e., −1.3 and −1.8 V vs SHE), the overpotential of the cell resulted minimized by the maintenance of the biological activity of the bioanode. Finally, during the last cathodic potentiostatic condition at − 2.3 V vs SHE, the loss of the biological activity and the establishment of the water oxidation reaction promoted an increase of the cell overpotentials.

3.4. CO_2 abatement and inorganic carbon mass balance

The MEC performance in terms of biogas upgrading (i.e., CO_2 abatement) at the cathode was evaluated by means of the inorganic carbon (IC) mass balance.

As reported in Fig. 4, the concentration of bicarbonate inside the cathodic chamber, where the CO_2 is absorbed, is significantly higher than the concentration inside the anodic chamber or inside the anodic feeding solution, with an average value of 2 g/L. The anodic concentration follows the cathodic trend due the migration and diffusion of the bicarbonate through the anion exchange membrane, resulting on average 1.6 g/L, a slightly lower value with respect to the cathodic bicarbonate concentration (Fig. S4). The detailed average concentrations of bicarbonate in each explored condition in the different liquid streams of the reactor are reported in Table S1 (supplementary materials). Considering the net difference in terms of bicarbonate concentration between anode influent and effluent, the net flux of bicarbonate from the cathode to the anode can be evaluated. As reported in Table 7, the diffusion of bicarbonate produced by cathodic CO_2 sorption through the AEM, represented the main CO_2 removal mechanism of the biocathode. Moreover, by the analysis of the inorganic carbon mass balance, the percentage of CO_2 transformed into methane resulted always around 5 − 7%, with the only exception for the −1.8 V operational period where the percentage increased to about 15%. Moreover, Table 7 shows the recovery of IC in the mass balance by considering both the two main removal mechanisms (i.e., CO_2 reduction into methane and bicarbonate migration) which overall accounted from about 30% to approximately 90% of the total removed IC. The bicarbonate transferred from the cathode to the anode, allowed for a contribution between 58 and 119 mA of the electroneutrality maintenance of the cell, demonstrating that is not the only anion responsible of the electroneutrality maintenance. The low recovery of inorganic carbon suggested the presence of undetected additional CO_2 removal mechanisms such as the precipitation of insoluble carbonate, i.e., magnesium/calcium carbonate (magnesium and calcium are present inside the mineral medium) promoted by the generation of alkalinity. In order to better understand the CO_2 removal mechanisms in the biocathode, a blank test was performed by interrupting the application of potential to the cathodic chamber while both liquid and gaseous influents have been maintained at the same flow

Table 6
Cell overpotential determination throughout the operating condition explored.

CONTROL OF THE ANODE POTENTIAL				CONTROL OF THE CATHODE POTENTIAL		
	2.55 gCOD/Ld	3.82 gCOD/Ld	5.11 gCOD/Ld	−1.3 V vs SHE	−1.8 vs SHE	−2.3 vs SHE
ΔV	−2.29	−2.35	−3.85	−1.82	−2.25	−4.18
$\Delta V_{(meas)}$	−1.52	−1.52	−2.72	−1.85	−2.27	−3.76
Ση	0.77	0.83	1.13	−0.03	−0.03	0.41

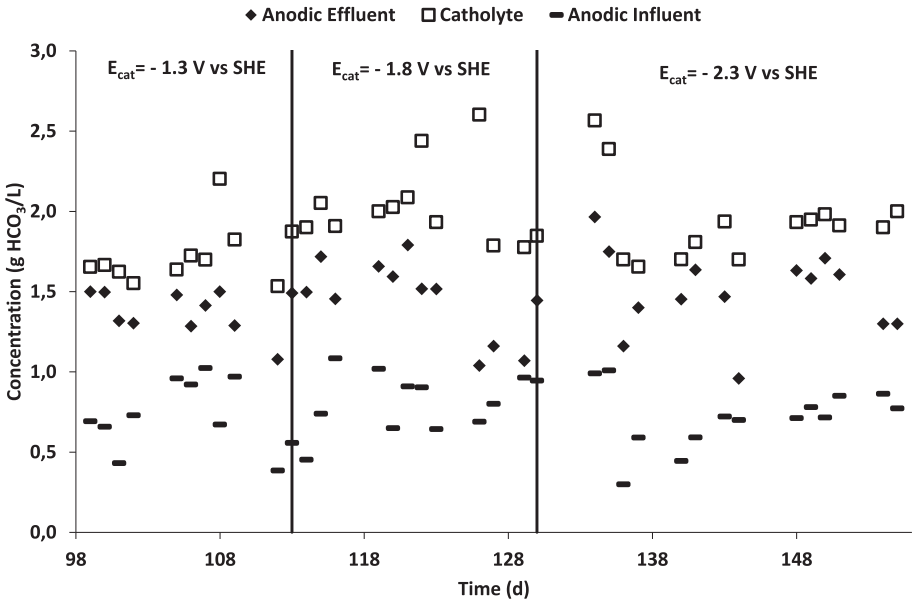

Fig. 4. Bicarbonate concentration inside the liquid phases during the cathodic potential control periods of the MEC.

Table 7
Inorganic Carbon mass balance during the different explored operating periods, including the CO_2 removal blank test.

E_{an}/E_{cath} (V vs SHE)	E_{an} + 0.2	E_{an} + 0.2	E_{an} + 0.2	E_{cath} −1.3	E_{cath} −1.8	E_{cath} −2.3	BLK
OLR (gCOD/Ld)	2.55	3.82	5.11	2.55	2.55	2.55	2.55
CO_2 removal (mmol/d)	249 ± 15	227 ± 12	166 ± 11	276 ± 16	215 ± 13	199 ± 12	79 ± 11
rCH_4 (mmol/d)	11 ± 1	16 ± 1	9 ± 1	12 ± 1	32 ± 2	15 ± 1	8 ± 1
$HCO_3^-{}_{transf}$ (mmol/d)	74 ± 1	70 ± 1	139 ± 3	63 ± 1	52 ± 1	107 ± 2	78 ± 3
$HCO_3^-{}_{transf}$ (mA)	83 ± 1	78 ± 1	155 ± 3	71 ± 1	58 ± 1	119 ± 2	–
Recovery (%)	34 ± 2	38 ± 1	89 ± 3	27 ± 3	39 ± 2	61 ± 1	99 ± 6

rates. During this operational period, in the cathodic chamber 79 ± 11 mmol/d of CO_2 were removed while 8 ± 1 mmol/d of methane were produced. It is important to notice that the cathodic methane production was obtained by the VFA diffusion from the anode to the cathode and was not related to the flowing current. During the blank test, the HCO_3^- concentration inside the cathodic chamber resulted 1.6 ± 0.1 g/L; while the influent and effluent HCO_3^- concentration in the anodic chamber resulted significantly different with an average concentration of 0.8 ± 0.1 and 1.5 ± 0.1 g/L, respectively. The bicarbonate transferred through the AEM justified 78 mmol/d of CO_2 giving a recovery of 99% considering that the methane production was driven only by the VFA consumption. The blank test clearly indicated that the

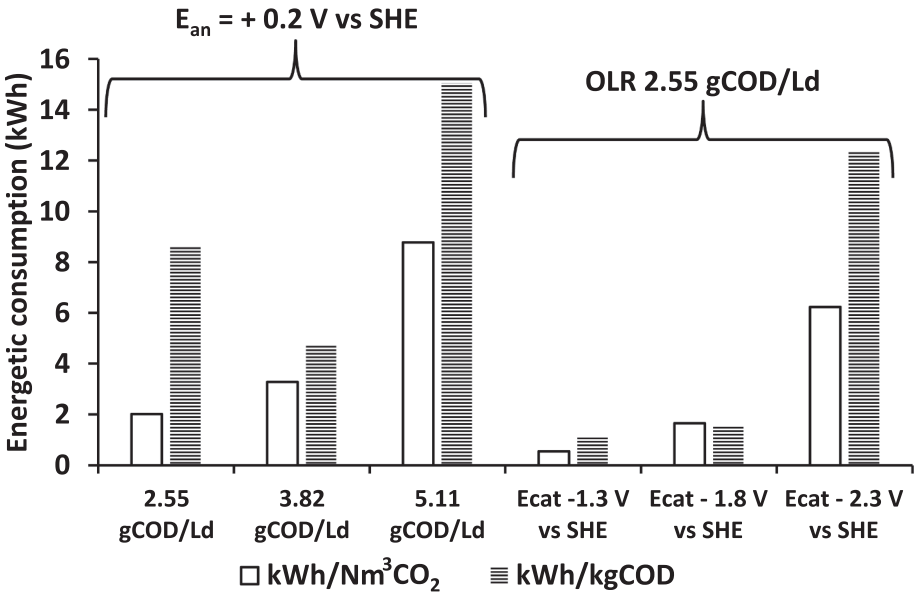

Fig. 5. Comparison of the MEC energetic consumptions during the six operating periods explored.

(bio)electrochemical process resulted responsible for a considerable amount of CO_2 removal which indicates that other additional CO_2 removal mechanisms are activated by the presence of additional electrochemical reactions with respect to bicarbonate migration and methane production.

3.5. Energetic consumptions

The MEC performance was also evaluated in terms of energetic consumption, whereby the energetic costs were evaluated for the two main performances of the MEC: the COD consumption and the CO_2 removal. To show how promising this technology is, each MEC operation was compared with a benchmark technology. Water scrubbing for biogas upgrading (expressed as normal m^3 of removed CO_2) and activated sludge for COD removal are the two technologies widely utilized. As reported in Fig. 5, the CO_2 removal power consumption increased along with the OLR during the anodic potentiostatic condition, the power consumption increase resulted in line with the increase of current and cell voltage necessary to operate the MEC. The shift of the potentiostatic control of the reactor from the anode to the cathode promoted a strong decrease of the energy consumption for CO_2 and COD removal. The power consumption decrease resulted described by the minimization of the anodic overpotential which was able to maintain the electrode microorganism interaction also during its counter electrode role. The two lower energetic consumption were obtained during the −1.3 V and the −1.8 V operational periods during which it was necessary only 0.6 and 1.7 kWh for every Nm^3 of CO_2, respectively (Table S2). On the contrary, the last cathodic potentiostatic condition was characterized by the higher energy consumption for CO_2 and COD removal. The result is attributed to the loss of the bioelectrochemical COD oxidation of the anode chamber which increases its potential probably for a kinetic limitation of the anodic reaction.

4. Conclusions

This study confirmed the possibility to simultaneously abate CO_2 from a gaseous mixture and remove COD from a liquid stream using a tubular micro-pilot MEC. The increase of the OLR from 2.55 gCOD/Ld to 3.82 and subsequently 5.11 gCOD/Ld, did, in fact, enhance the electric current from 240 ± 16 mA to 312 ± 28 mA devoid of performances' improvement. Regarding the CO_2 removal mechanisms, the experimental study permitted to underline the presence of additional CO_2 removal mechanisms not identified in previous research conducted in a different scale and geometry which will need specific investigations for their quantification. The most interesting result of the present paper is the confirmation at a different scale and geometry of the possibility to switch the potentiostatic control of the MEC from the anode to the cathode. Indeed, after the OLR effect characterisation under anodic potentiostatic control (at + 0.2 V vs. the Standard Hydrogen electrode, SHE), the potential control was switched from the anode to the cathode electrode (controlled at −1.3 V, −1.8 V, or −2.3 V vs. SHE) and, as expected, the decrease of the energy consumption of the MEC was obtained. This energy consumption decrease was driven by the anodic reaction overpotential reduction from 0.88 V to 0.43 V maintaining a sufficient reaction rate for the anodic and cathodic bioelectrochemical reaction (3.1 gCOD/d and 12 mmolCH_4/d). Indeed, the methane production rate reached 32 ± 2 mmol/d during the −1.8 V vs SHE period, the COD removal was the highest (5.2 ± 0.1 gCOD/d) during the same period. However, pushing the cathodic potential to −2.3 V vs SHE had a negative effect on process energy consumption due to establishment of the water oxidation reaction in the anodic chamber which required a considerable higher potential. The working electrode switch from the anode to the cathode confirmed to be a promising solution to minimize the energetic consumptions of the process, which allowed to obtain lower energy consumption with respect to the benchmark technologies' consumption: activated sludge (1.1 ± 1 vs 1.2 kWh/kgCOD) for COD removal and water scrubbing for biogas upgrading (0.6 ± 1 vs 0.8 kWh/Nm^3CO_2). The interesting MEC performances highlighted by the experimental study showed the effectiveness of the integrated bioelectrochemical process in which low-COD streams can be adopted as electron source to sustain the CO_2 conversion into CH_4. Thus, the proceeding of the electron flow promoted the additional removal of the CO_2 due to the spontaneous alkalinity generation in the cathodic chamber derived from the ionic transport of different anions. Despite several issues are currently present in the optimization of the technology energy consumption, the studied bioelectrochemical process represents a flexible, eco-friendly and effective technology which can significantly contribute to the optimization of the anaerobic digestion process.

Declaration of Competing Interest

The authors declare that they have no known competing financial interests or personal relationships that could have appeared to influence the work reported in this paper.

Acknowledgments

Cristina Porcu is acknowledged for his skilful assistance in the experimental activity "This project has received funding from the European Union's Horizon 2020 research and innovation program under grant agreement No 688338 (No Agricultural Waste- NoAw project)"

Appendix A. Supplementary data

Supplementary data to this article can be found online at https://doi.org/10.1016/j.cej.2021.131909.

References

[1] W. Zappa, M. Junginger, M. van den Broek, Is a 100% renewable European power system feasible by 2050? Appl. Energy. 233–234 (2019) 1027–1050, https://doi.org/10.1016/j.apenergy.2018.08.109.
[2] J.A. Martens, A. Bogaerts, N. DeKimpe, P.A. Jacobs, G.B. Marin, K. Rabaey, M. Saeys, S. Verhelst, The chemical route to a carbon dioxide neutral world, ChemSusChem 10 (6) (2017) 1039–1055, https://doi.org/10.1002/cssc.201601051.
[3] A. Mattioli, G.B. Gatti, G.P. Mattuzzi, F. Cecchi, D. Bolzonella, Co-digestion of the organic fraction of municipal solid waste and sludge improves the energy balance of wastewater treatment plants: rovereto case study, Renew. Energy. 113 (2017) 980–988, https://doi.org/10.1016/j.renene.2017.06.079.
[4] E. Ryckebosch, M. Drouillon, H. Vervaeren, Techniques for transformation of biogas to biomethane, Biomass Bioenergy 35 (5) (2011) 1633–1645, https://doi.org/10.1016/j.biombioe.2011.02.033.
[5] F. Bauer, T. Persson, C. Hulteberg, D. Tamm, Biogas upgrading - technology overview, comparison and perspectives for the future, Biofuels Bioprod. Biorefining. 7 (5) (2013) 499–511, https://doi.org/10.1002/bbb.2013.7.issue-510.1002/bbb.1423.
[6] S.N.B. Villadsen, P.L. Fosbøl, I. Angelidaki, J.M. Woodley, L.P. Nielsen, P. Møller, The potential of biogas; the solution to energy storage, ChemSusChem 12 (10) (2019) 2147–2153, https://doi.org/10.1002/cssc.v12.1010.1002/cssc.201900100.
[7] N. Scarlat, J.F. Dallemand, F. Fahl, Biogas: developments and perspectives in Europe, Renew. Energy. 129 (2018) 457–472, https://doi.org/10.1016/j.renene.2018.03.006.
[8] P. Nikolaidis, A. Poullikkas, A comparative overview of hydrogen production processes, Renew. Sustain. Energy Rev. 67 (2017) 597–611, https://doi.org/10.1016/j.rser.2016.09.044.
[9] I. Angelidaki, L. Treu, P. Tsapekos, G. Luo, S. Campanaro, H. Wenzel, P.G. Kougias, Biogas upgrading and utilization: current status and perspectives, Biotechnol. Adv. 36 (2) (2018) 452–466, https://doi.org/10.1016/j.biotechadv.2018.01.011.
[10] U. Schröder, F. Harnisch, L.T. Angenent, Microbial electrochemistry and technology: terminology and classification, Energy Environ. Sci. 8 (2) (2015) 513–519, https://doi.org/10.1039/C4EE03359K.
[11] M. Zeppilli, E. Dell'Armi, L. Cristiani, M.P. Papini, M. Majone, Reductive/oxidative sequential bioelectrochemical process for perchloroethylene removal, Water (Switzerland). 11 (2019), https://doi.org/10.3390/w11122579.
[12] L. Cristiani, M. Zeppilli, C. Porcu, M. Majone, Ammonium Recovery and Biogas Upgrading in a Tubular Micro-Pilot Microbial Electrolysis (2020), https://doi.org/10.3390/molecules25122723.
[13] S.M.T. Raes, L. Jourdin, C.J.N. Buisman, D.P.B.T.B. Strik, Continuous long-term bioelectrochemical chain elongation to butyrate, ChemElectroChem. 4 (2) (2017) 386–395, https://doi.org/10.1002/celc.201600587.

[14] T. Sangeetha, Z. Guo, W. Liu, M. Cui, ScienceDirect Cathode material as an influencing factor on beer wastewater treatment and methane production in a novel integrated upflow microbial electrolysis cell, Int. J. Hydrogen Energy. 41 (2015) 2189–2196, https://doi.org/10.1016/j.ijhydene.2015.11.111.
[15] M.T. Noori, M.T. Vu, R.B. Ali, B. Min, Recent advances in cathode materials and configurations for upgrading methane in bioelectrochemical systems integrated with anaerobic digestion, Chem. Eng. J. 392 (2020) 123689, https://doi.org/10.1016/j.cej.2019.123689.
[16] K. Zhou, S. Chaemchuen, F. Verpoort, Alternative materials in technologies for Biogas upgrading via CO2capture, Renew. Sustain. Energy Rev. 79 (2017) 1414–1441, https://doi.org/10.1016/j.rser.2017.05.198.
[17] R. Lacroix, S.D. Silva, M.V. Gaig, R. Rousseau, M.-L. Délia, A. Bergel, Modelling potential/current distribution in microbial electrochemical systems shows how the optimal bioanode architecture depends on electrolyte conductivity, Phys. Chem. Chem. Phys. 16 (41) (2014) 22892–22902, https://doi.org/10.1039/C4CP02177K.
[18] M. Oliot, P. Chong, B. Erable, A. Bergel, Influence of the electrode size on microbial anode performance, Chem. Eng. J. 327 (2017) 218–227, https://doi.org/10.1016/j.cej.2017.06.044.
[19] S. Saheb-Alam, A. Singh, M. Hermansson, F. Persson, A. Schnürer, B.-M. Wilén, O. Modin, H.L. Drake, Effect of start-up strategies and electrode materials on carbon dioxide reduction on biocathodes, Appl. Environ. Microbiol. 84 (4) (2018), https://doi.org/10.1128/AEM.02242-17.
[20] F. Aulenta, P. Reale, A. Canosa, S. Rossetti, S. Panero, M. Majone, Characterization of an electro-active biocathode capable of dechlorinating trichloroethene and cis-dichloroethene to ethene, Biosens. Bioelectron. 25 (7) (2010) 1796–1802, https://doi.org/10.1016/j.bios.2009.12.033.
[21] L. Wang, Z. He, Z. Guo, T. Sangeetha, C. Yang, L. Gao, A. Wang, W. Liu, Microbial community development on different cathode metals in a bioelectrolysis enhanced methane production system, J. Power Sources. 444 (2019) 227306, https://doi.org/10.1016/j.jpowsour.2019.227306.
[22] M. Zeppilli, M. Simoni, P. Paiano, M. Majone, Two-side cathode microbial electrolysis cell for nutrients recovery and biogas upgrading, Chem. Eng. J. 370 (2019) 466–476, https://doi.org/10.1016/j.cej.2019.03.119.
[23] L. Wang, C. Yang, T. Sangeetha, Z. He, Z. Guo, L. Gao, A. Wang, W. Liu, Methane production in a bioelectrochemistry integrated anaerobic reactor with layered nickel foam electrodes, Bioresour. Technol. 313 (2020) 123657, https://doi.org/10.1016/j.biortech.2020.123657.
[24] H. Beyenal, SYSTEMS BIOFILMS IN From Laboratory Practice to Data, n.d.
[25] M. Zeppilli, P. Paiano, C. Torres, D. Pant, A critical evaluation of the pH split and associated effects in bioelectrochemical processes, Chem. Eng. J. 422 (2021) 130155, https://doi.org/10.1016/j.cej.2021.130155.
[26] M. Zeppilli, A. Lai, M. Villano, M. Majone, Anion vs cation exchange membrane strongly affect mechanisms and yield of CO2fixation in a microbial electrolysis cell, Chem. Eng. J. 304 (2016) 10–19, https://doi.org/10.1016/j.cej.2016.06.020.
[27] M. Zeppilli, L. Cristiani, E. Dell'Armi, M. Majone, Bioelectromethanogenesis reaction in a tubular Microbial Electrolysis Cell (MEC) for biogas upgrading, Renew. Energy. 158 (2020) 23–31, https://doi.org/10.1016/j.renene.2020.05.122.
[28] M. Zeppilli, P. Paiano, M. Villano, M. Majone, Anodic vs cathodic potentiostatic control of a methane producing microbial electrolysis cell aimed at biogas upgrading, Biochem. Eng. J. 152 (2019) 107393, https://doi.org/10.1016/j.bej.2019.107393.
[29] M. Zeppilli, L. Cristiani, E. Dell'Armi, M. Villano, Potentiostatic vs galvanostatic operation of a Microbial Electrolysis Cell for ammonium recovery and biogas upgrading, Biochem. Eng. J. 167 (2021) 107886, https://doi.org/10.1016/j.bej.2020.107886.